



## UvA-DARE (Digital Academic Repository)

### Atomic spin-chain realization of a model for quantum criticality

Toskovic, R.; van den Berg, R.; Spinelli, A.; Eliens, I.S.; van den Toorn, B.; Bryant, B.; Caux, J.-S.; Otte, A.F.

**DOI**

[10.1038/NPHYS3722](https://doi.org/10.1038/NPHYS3722)

**Publication date**

2016

**Document Version**

Other version

**Published in**

Nature Physics

**License**

Article 25fa Dutch Copyright Act (<https://www.openaccess.nl/en/in-the-netherlands/you-share-we-take-care>)

[Link to publication](#)

**Citation for published version (APA):**

Toskovic, R., van den Berg, R., Spinelli, A., Eliens, I. S., van den Toorn, B., Bryant, B., Caux, J.-S., & Otte, A. F. (2016). Atomic spin-chain realization of a model for quantum criticality. *Nature Physics*, 12(7), 656-660. <https://doi.org/10.1038/NPHYS3722>

**General rights**

It is not permitted to download or to forward/distribute the text or part of it without the consent of the author(s) and/or copyright holder(s), other than for strictly personal, individual use, unless the work is under an open content license (like Creative Commons).

**Disclaimer/Complaints regulations**

If you believe that digital publication of certain material infringes any of your rights or (privacy) interests, please let the Library know, stating your reasons. In case of a legitimate complaint, the Library will make the material inaccessible and/or remove it from the website. Please Ask the Library: <https://uba.uva.nl/en/contact>, or a letter to: Library of the University of Amsterdam, Secretariat, Singel 425, 1012 WP Amsterdam, The Netherlands. You will be contacted as soon as possible.

*UvA-DARE is a service provided by the library of the University of Amsterdam (<https://dare.uva.nl>)*

# Atomic spin-chain realization of a model for quantum criticality

R. Toskovic<sup>1</sup>, R. van den Berg<sup>2</sup>, A. Spinelli<sup>1</sup>, I. S. Eliens<sup>2</sup>, B. van den Toorn<sup>1</sup>, B. Bryant<sup>1</sup>, J.-S. Caux<sup>2</sup> and A. F. Otte<sup>1</sup>

<sup>1</sup>Department of Quantum Nanoscience, Kavli Institute of Nanoscience, Delft University of Technology, Lorentzweg 1, 2628 CJ Delft, The Netherlands

<sup>2</sup>Institute for Theoretical Physics, University of Amsterdam, Science Park 904, 1090 GL Amsterdam, The Netherlands

## Rate equations

The theoretical simulations are based on (1), and summarized here for completeness. To model the differential conductance we have used rate equations up to third order in the coupling between the conduction electrons and the Co atoms. The transition probability for an electron tunneling from tip to sample from a collective initial state (i) to a final state (f) is given by

$$W_{if} = \frac{2\pi}{\hbar} \left[ |H'_{if}|^2 + \sum_m \left( \frac{H'_{im}H'_{mf}H'_{fi}}{E_i - E_m} + c.c. \right) \right] \delta(E_i - E_j)$$

where  $H'$  represents the (isotropic) interaction between the Co atoms and the conduction electrons in the tip and substrate. We assume that the only non-negligible current flows through the atom directly situated under the tip, indicated with an index  $l$  for the spin exchange operators hereafter. The interaction Hamiltonian is thus given by

$$H' = \sum_{\alpha, \alpha'} \sum_{k, k'} J^{\alpha\alpha'} \left[ S_l^z \left( c_{\alpha l k' \uparrow}^\dagger c_{\alpha k \uparrow} - c_{\alpha l k' \downarrow}^\dagger c_{\alpha k \downarrow} \right) + S_l^+ c_{\alpha l k' \downarrow}^\dagger c_{\alpha k \uparrow} + S_l^- c_{\alpha l k' \uparrow}^\dagger c_{\alpha k \downarrow} \right] + \sum_{\alpha, \alpha'} \sum_{k, k'} \sum_{\sigma} T^{\alpha\alpha'} c_{\alpha l k' \sigma}^\dagger c_{\alpha k \sigma}$$

where the indices  $\alpha$  and  $\alpha'$  represent either the tip or substrate, such that  $T^{\text{ts}}$  and  $J^{\text{ts}}$  are the coupling constants for potential scattering and spin flip exchange processes respectively involving electrons from both the tip and the substrate. The second order contribution to the differential conductance then yields

$$\frac{\partial I^{(2)}}{\partial V} = \frac{2\pi e^2}{\hbar} \rho^t \rho^s \left( 2 (T^{\text{ts}})^2 + (J^{\text{ts}})^2 \sum_{if} p_i(T) \left[ |\langle \varepsilon_f | S_l^+ | \varepsilon_i \rangle|^2 + |\langle \varepsilon_f | S_l^- | \varepsilon_i \rangle|^2 + 2 |\langle \varepsilon_f | S_l^z | \varepsilon_i \rangle|^2 \right] \right. \\ \left. \times [\Theta(eV + \Delta_{if}, T) + \Theta(-eV + \Delta_{if}, T)] \right)$$

with the usual temperature broadened step function

$$\Theta(\omega) = (1 - (\omega/k_B T + 1) \exp(-\omega/k_B T)) / (1 - \exp(-\omega/k_B T))^2$$

and  $\Delta_{if} = \varepsilon_i - \varepsilon_f$  the energy difference between the eigenstates  $i$  and  $f$  of  $H_{3/2}$  in the manuscript. The parameters  $\rho^t$  and  $\rho^s$  are the density of states of the tip and substrate electrons at the Fermi energy. We have assumed the thermal equilibrium solution for the stationary level occupations  $p_i(T)$ , justified by the fact that the measurements are performed with a large distance between the tip and sample.

The largest third order contribution to the differential conduction arises due to interference between electrons tunneling from tip to substrate and spin exchange processes between the substrate electrons and the Co atoms, yielding

$$\frac{\partial I^{(3)}}{\partial V} = \frac{4\pi e^2}{\hbar} \rho^t \rho^s (J^{ts})^2 (\rho^s J^{ss}) \sum_{if} p_i(T) \sum_{\substack{\alpha, \beta, \gamma = \\ +, -, z}}^m \varepsilon_{\alpha\beta\gamma} \langle \varepsilon_i | S_i^\alpha | \varepsilon_f \rangle \langle \varepsilon_f | S_f^\beta | \varepsilon_m \rangle \langle \varepsilon_m | S_m^\gamma | \varepsilon_i \rangle \times \\ (\Theta(eV + \Delta_{if}) [F(eV - \Delta_{fm}) + F(eV - \Delta_{mi})] + \Theta(-eV + \Delta_{if}) [F(-eV - \Delta_{fm}) + F(-eV - \Delta_{mi})])$$

where the Levi-Civita symbol  $\varepsilon_{\alpha\beta\gamma}$  has the value +1 for  $\varepsilon_{+-z}$  and all cyclic permutations, and the value -1 for all anti-cyclic permutations. The function  $F(\omega)$  is defined as

$$F(\omega) = - \int \int d\epsilon d\epsilon' \frac{\partial}{\partial \omega} f(\epsilon - \omega) \frac{f(\epsilon')}{\epsilon' - \epsilon} \approx \log \left| \frac{E_0 + |\omega|}{\omega + i\alpha k_B T} \right|$$

where the last approximation is valid at low temperatures. The parameter  $\alpha$  represents the thermal broadening of the Fermi Dirac distributions  $f(\epsilon)$  and is set to 1.5 throughout the computations. The value of the dimensionless parameter  $\rho^s J^{ss}$  was previously estimated (2) to be equal to  $\rho^s J^{ss} \approx 0.15$ , and as such is used in the theoretical modeling.

Throughout the paper we have used an effective temperature of 800 mK, which is higher than the base temperature of the STM due to the voltage modulations present in the experiment. All theoretical calculations of the differential conductance have been normalized by their value at 7.8 mV. We have furthermore set the ratio between the spin exchange constant and the potential scattering coupling to  $J^{ts} / T^{ts} \approx 0.47$  in order to match the zero bias  $dI/dV$  approximately with the experimental values.

For the calculation of the differential conductance in the effective spin-1/2 model, the Schrieffer-Wolff transformation yields the effective Hamiltonian describing the spin-1/2 multiplet of the Co chain. However, it is worth noting that the Kondo exchange interaction also changes due to the projection onto the spin-1/2 sector of the Co atoms. In contrast to the expansion of the Hamiltonian describing the Co chain, where we have expanded up to first order in  $1/D$ , we have for simplicity only taken into account the zeroth order expansion in  $1/D$  for the exchange with the conduction electrons, leading to an extra factor of 2 in front of the  $S^+$  and  $S^-$  terms in  $H'$ . The effective spin-1/2 Kondo exchange thus becomes anisotropic. Finally, the spin-1/2  $dI/dV$  curves are normalized by the  $dI/dV$  values at 7.8 mV of the spin-3/2 computations.

## Supplementary figures

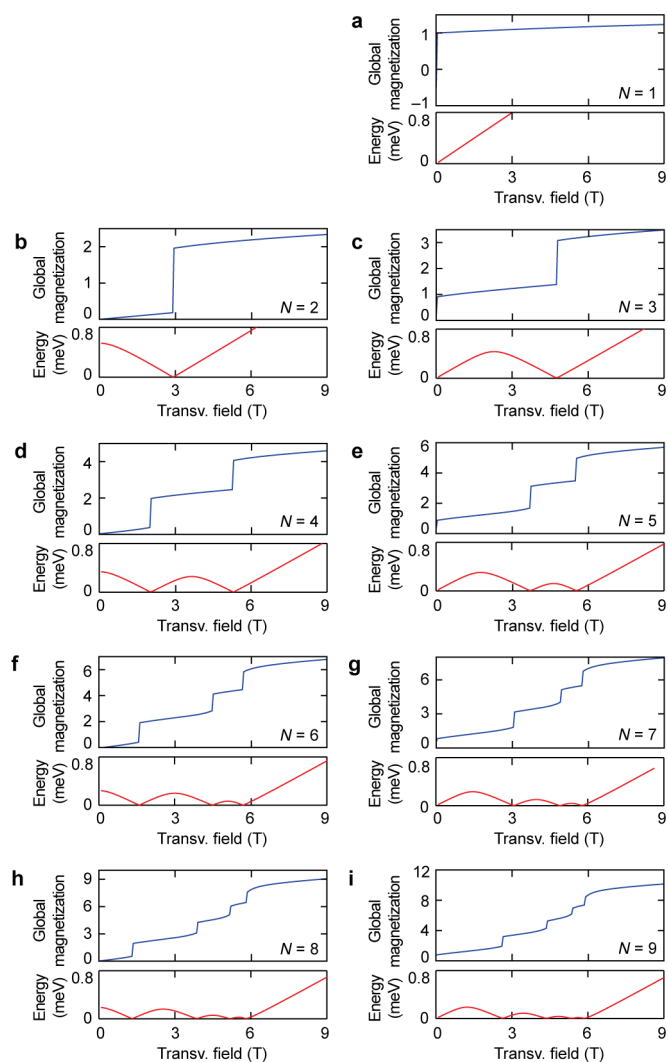


**Fig. S1.** a—i. Total magnetization calculations along the field direction (blue) for chains  $N = 1$  to 9 as calculated from the  $H_{3/2}$  model. Below: lowest excitation energy calculations (red) following from the same model.

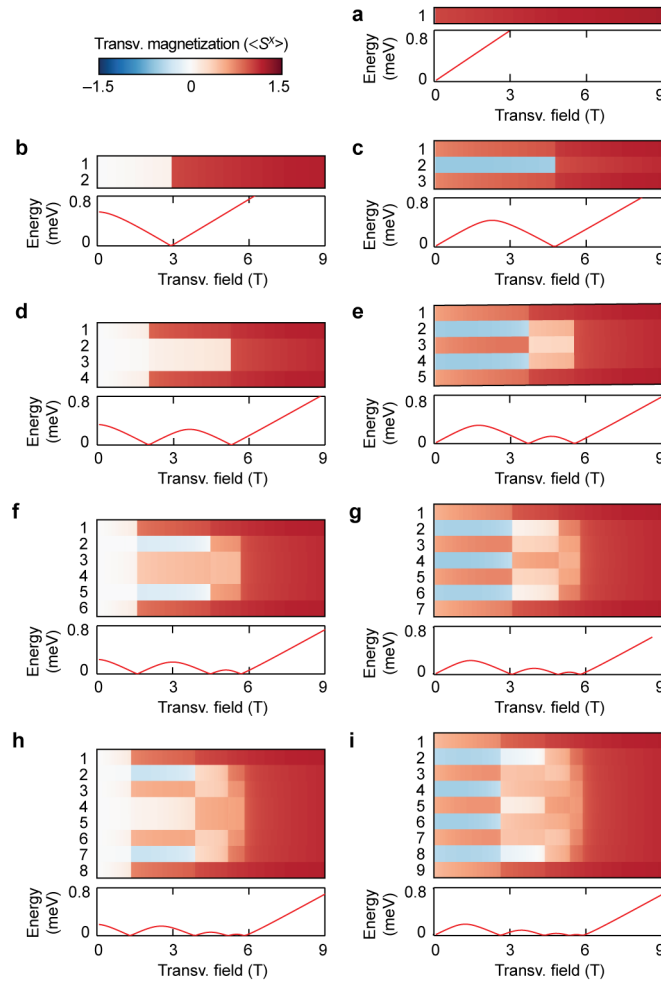


**Fig. S2. a—i.** Calculated magnetization ( $\langle S^x \rangle$ ) for the  $H_{3/2}$  model along the field direction per site for  $N = 1$  to  $9$  chains. Each magnetization plot is accompanied with the  $H_{3/2}$  lowest excitation energy curve (red). Changes in local magnetization correspond to the experimentally observed field evolution of  $dI/dV$  features per site shown in Figs. 3 and S3.

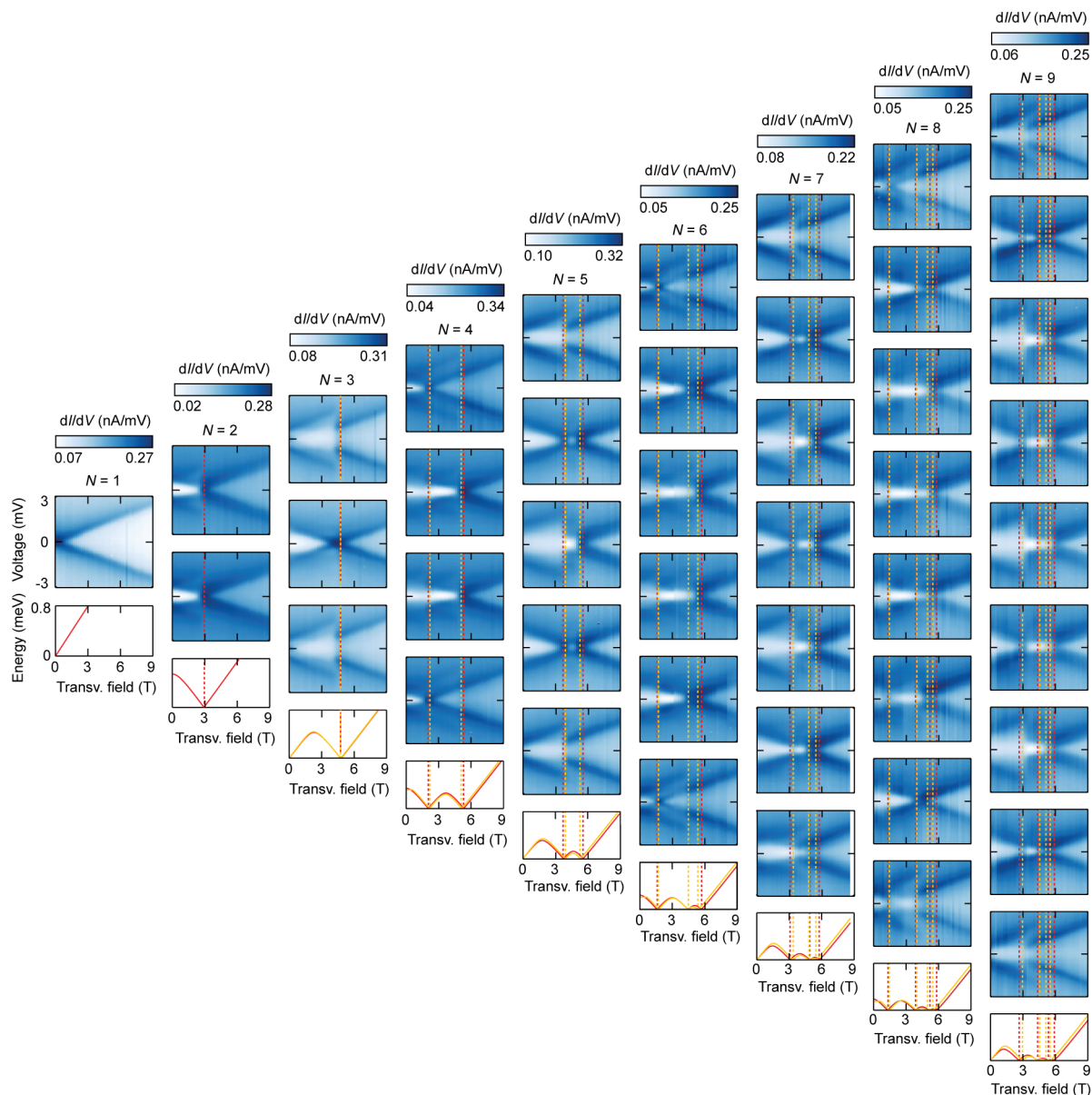


**Fig. S3.** Experimental results on chains of 1 to 9 atoms – comparison with  $H_{3/2}$  taking into account next-nearest neighbor (nnn) interaction.  $\pm 3$  mV IETS spectra from 0 T to 9 T transverse field (in 200 mT increments) obtained on each atom of every chain up to a length of 9 atoms (up to 8.6 T for  $N = 7$ ). Red dashed lines indicate positions of expected ground state crossings calculated from the  $H_{3/2}$  model with antiferromagnetic nn coupling  $J$  only (same as in Fig. 3b). Orange dashed lines come from the same model but accounting for ferromagnetic nnn coupling of  $0.05J$ . Same color coding applies to the energy calculations below each chain data set. Due to normalization, scaling of individual spectra may differ by  $\sim 20\%$  from values listed at the color bars.

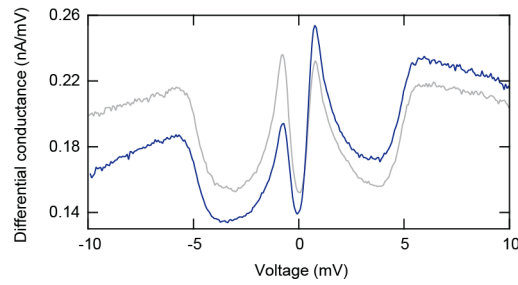


**Fig. S4.** IETS spectra on a single Co atom on Cu<sub>2</sub>N in a 3 T magnetic field oriented perpendicular to the surface, taken with the same spin-polarized tip as used in Fig. 4 (blue) and with a spin-unpolarized tip (grey).

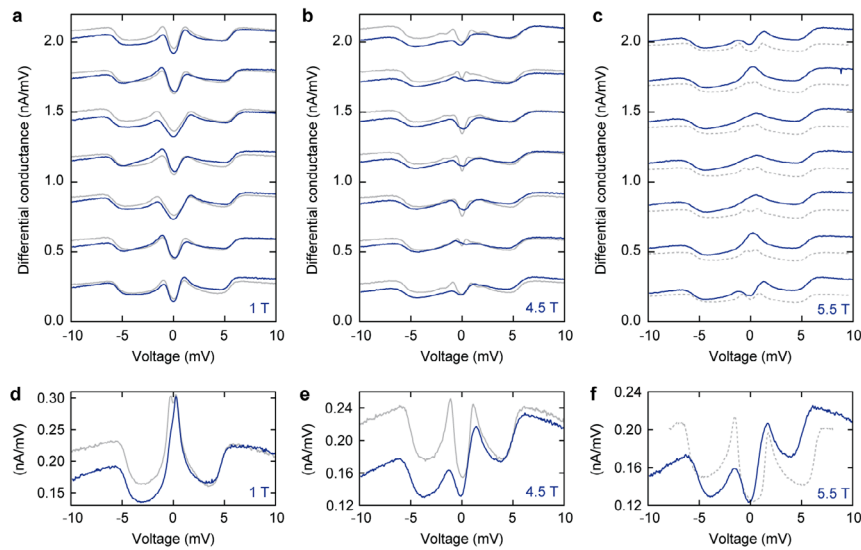


**Fig. S5.** **a–c.** Spin-polarized IETS spectra taken at 1 T, 4.5 T and 5.5 T transverse field in an  $N = 7$  chain (blue curves). Corresponding spectra taken with an unpolarized tip are shown in grey. **d–e.** IETS spectra taken on a single Co atom at the same field values as in **a–c** with the same spin-polarized tip (blue) and with a spin-unpolarized tip (grey). Dashed spin-unpolarized curves were taken on a different instance of the chain/atom than the corresponding spin-polarized curves.

**References**

1. M. Ternes, Spin excitations and correlations in scanning tunneling spectroscopy. *New J. Phys.* **17**, 063016 (2015).
2. A. Spinelli *et al.*, Exploring the phase diagram of the two-impurity Kondo problem. *Nat. Commun.* **6**, 10046 (2015).